Laser-Desorption Mass Spectrometry of Standard Polynuclear Aromatic Hydrocarbons and Fullerenes

Alan A. Herod,[*,a] **Brian J. Stokes,**[b] **Paul Hancock,**[b] **Rafael Kandiyoti,**[a] **John E. Parker,**[c] **Chris A. F. Johnson,**[c] **Philip John**[c] **and Gerry Smith**[c]
[a] *Department of Chemical Engineering and Chemical Technology, Imperial College, University of London, London, UK SW7 2BY*
[b] *British Coal Corporation, Coal Research Establishment, Stoke Orchard, Cheltenham, Glos., UK GL52 4RZ*
[c] *Department of Chemistry, Heriot-Watt University, Riccarton, Edinburgh, UK EH14 4AS*

Laser-desorption mass spectrometry (LD–MS) has been used to investigate the mass spectra of a suite of standard polynuclear aromatic hydrocarbons and a sample of fullerenes (mixed C_{60} and C_{70}), as a part of a study of high molecular mass ions in tars and liquid extracts derived from coal. Positive- and negative-ion LD–MS spectra of these standards were compared with electron impact spectra to elucidate the mechanism of laser desorption. The data indicate that ion–molecule reactions occur during the desorption step giving hydrogenated molecular ions *via* mechanisms analogous to self-chemical ionization; fullerenes gave no hydrogenated molecular ions. Carbon cluster ions (both positive and negative ions) are formed by the laser energy with fewer carbon atoms than the original molecule, suggesting their formation to result from the thermal destruction of parent molecules. However, none of the standard compounds gave cluster ions greater than the hydrogenated molecular ions. This finding provides confirmation that large molecular mass materials identified in coal-derived liquids originated from the sample itself and did not form from smaller molecular mass compounds under the power of the laser.

Laser desorption mass spectrometry has been used for the analysis of biological molecules as well as pure polynuclear aromatic hydrocarbons and other standards. Matrix assisted laser desorption mass spectrometry has been reviewed recently;[1,2] biomolecules give mainly M^+ with some $(M + H)^+$ while polymers give positive ion M^+ spectra.[3] In matrix assisted desorption, the role of the matrix is to absorb the laser energy and generate molecular ions from the sample without contributing significantly to the ionization itself. It has been noted[4] that the matrix technique is of no use if the sample absorbs at the laser frequency as well as the matrix.

The single laser method, in which desorption and ionization take place as a consequence of a single laser pulse, has been used by many groups. Rhodamine B gave a molecular ion with no fragmentation.[5] Direct laser desorption of thin-layer chromatography spots of polynuclear aromatic hydrocarbons gave molecule cations[6,7] and in one study,[8] $(M - H)^-$ ions were observed from phthalic acid with some fragmentation information in the positive ion spectra. The role of the thin layer material in direct laser desorption has been reviewed.[9] Polynuclear aromatic hydrocarbons deposited on a target have been observed[10] to give M^+ ions as well as $(M + Na)^+$ ions when mixed with NaCl. Both M^+ and $(M + H)^+$ ions have been detected from polynuclear aromatics,[11] while the negative ion mode gave $(M - H)^-$, $(M - 2H)^-$ and $(M - 3H)^-$ ions. Mixtures of polynuclear aromatic hydrocarbons examined by laser desorption ion trap mass spectrometry[12] gave association ions in the negative ion mode and M^+ ions in the positive ion mode; in that study, the buffer gas, helium, may have contributed to stabilization of the negative-ion association ions. Fullerenes have also been examined by laser desorption[13] and by laser desorption–chemical ionization (LD–MS),[14] giving M^+ and $(M + H)^+$ ions in the two techniques respectively.

The double laser technique, in which one laser ablates material from a solid surface producing a molecular beam of neutral molecules which are then subjected to multiphoton ionization by the second laser, has been recently reviewed.[15] The advantages to be gained by separating the ablation and ionization steps are considerable and include the avoidance of pyrolysis of the sample. The double laser technique has been used[16,17] to produce molecular ions M^+ from hydrocarbons in meteoritic material.

In our work,[18-20] we have used a single laser at low power to both desorb and ionize molecular ions from coal tars and extracts. We found considerably larger molecular ions (up to 12,000 u) than had hitherto been identified in coal derived material by laser desorption mass spectrometry (about 1200 u). In the present part of the study, we have examined standard hydrocarbons including fullerite, to demonstrate that the laser-desorption mechanism produced only molecular or pseudo-molecular ions under the conditions used and that no high mass cluster ions were formed by the laser. This aspect of the work is reported here.

Experimental

The instrument used for the laser desorption study was a LIMA 401L time-of-flight mass spectrometer from Cambridge Mass Spectrometry. A Nd-YAG laser, Q switched and operating at 266 nm was used for laser desorption. A defocused beam was used to obtain spectra from the sample which was mounted on an aluminium stub. The target was prepared by depositing about 50 mm^3 of a solution of the sample dissolved in toluene or benzene or their perdeuterio-derivatives, on the 25 mm diameter aluminium stub. The solvent was evaporated and then pumped by a turbo-molecular pump to remove the last traces of solvent. The effect of a liquid target, glycerol, on the spectrum was investigated using one of the aromatics, rubicene. Sinapinic acid,† one of the usual matrices used for matrix assisted laser

---

† 3,5-Dimethoxy-4-hydroxycinnamic acid.

desorption, was used to generate spectra from benzo[*e*]pyrene, dibenzopyrene and rubicene, in order to observe differences attributable to the matrix. The laser beam diameter of 2 to 5 μm allowed several spectra to be generated from one target using low to medium laser power to desorb and ionize rather than pyrolyze the aromatics.

The effect on the positive ion spectra of two compounds (benzo[*e*]pyrene and dibenzopyrene) of varying the laser power at the target surface was investigated by the simple expedient of allowing the topography of the crystalline sample surface (sample layer thickness) to change the effective laser spot diameter. With a constant laser power, slight but non-quantifiable changes in the diameter of the spot caused slight but significant changes in power; clearly the smaller the spot diameter, the greater was the effective laser power. Most of the spectra collected were of positive ions but for each aromatic, a negative ion spectrum was collected as well. The spectra collected correspond to a single laser shot; the signal to noise ratio would be improved by a spectral summation method but this is not available with the current instrument. However, for benzo[*e*]pyrene, dibenzopyrene and rubicene, ten or more spectra have been summed manually over the molecular ion region. This procedure produces no qualitative change in the spectrum but reduces the effect of variability in effective incident laser fluence from shot to shot caused by changes in sample topography.*

Electron impact spectra were generated for comparison, using a Kratos Concept S double focusing mass spectrometer, using 70 eV ionizing energy, with sample introduction either by the standard solids injection probe, heated up to 350 °C or by the gas chromatography inlet for lower molecular mass components. Positive ion spectra were recorded and compared with literature spectra where possible.

Compounds examined were phenanthrene (1), *m*/*z* 178, $C_{14}H_{10}$; pyrene (1) *m*/*z* 202, $C_{16}H_{10}$; chrysene (1) *m*/*z* 228, $C_{18}H_{12}$; benzo[*e*]pyrene (3) *m*/*z* 252, $C_{20}H_{12}$; dibenzopyrene (4) *m*/*z* 302, $C_{24}H_{14}$; rubicene (1) *m*/*z* 326, $C_{26}H_{14}$; pyranthrene (2) *m*/*z* 376, $C_{30}H_{16}$; rubrene† (2) *m*/*z* 532, $C_{42}H_{28}$; and fullerite (2), a nominal 10:1 mix of C_{60} and C_{70}, *m*/*z* 720 and 840: suppliers were Koch-Light (1), Aldrich Chemicals (2), Pfalz and Bauer (3) and BCR, Brussels (4).

Results and Discussion

The spectra of the aromatic compounds acquired by laser desorption show two features; (a) a series of peaks about the molecular ion mass and (b) a series of lower mass peaks corresponding to carbon clusters of the type C_nH_m, where *n* is less than the number of carbon atoms in the molecule and *m* can be 1, 2 or 3. Below, the molecular ion region peaks are considered before the carbon clusters.

In terms of the proportion of total ionization in the molecular ion region, at the highest effective energy, the molecular ion intensities are less than 1% while at the lowest effective energies, the molecular ion intensity can exceed 50% of total ionization.

The positive molecular ion regions of LD–MS spectra have been summarized in Tables 1 and 2, showing the equivalent molecular ion peaks by electron impact ionization. In Table 1, the relative proportions of the molecular ion peaks in the laser desorption mass spectra, from $(M - H)^+$ to $(M + 7H)^+$ are shown; the most intense of the peaks has been set to 100% in each case. For three compounds, benzo[*e*]pyrene, dibenzopyrene and rubicene, a number of spectra (10, 10 and 13 respectively) have been summed manually, and are shown in Table 1. We interpret the observation of ions from $(M + H)^+$ to $(M + 7H)^+$ in terms of ion–molecule reactions leading to reduction of the molecules by consecutive hydrogen atom additions, which occur in the gas-phase plume of desorbed material at relatively high local pressure; in desorption ionization methods this mechanism has been termed[21] reaction within the 'selvedge'. In the SIMS of organic materials, the addition of up to 8 hydrogen atoms and a proton has been observed[21] in the 'selvedge' as the $(M + 9H)^+$ ion. If this explanation is correct, then the reaction mechanism would appear to be very sensitive to laser energy changes; as noted above, laser energy absorbed by the sample may also be changed by variations in sample topography and sample thickness.

The changes in the molecular ion region of benzo[*e*]pyrene and dibenzopyrene with laser power are illustrated in Figs. 1 and 2 respectively. These show that as the laser power increases, the intensities of the molecular and pseudo molecular ions decrease and shift to lower mass, by a reduction in the number of added hydrogen atoms, towards the molar mass. In Fig. 1, only slight changes are evident between spectra (*a*) and (*b*), corresponding to shifts of relative intensity of the *m*/*z* 254 and 255 peaks and disappearance of *m*/*z* 257; at the highest energy, spectrum (*c*), only two ions at low intensity are apparent at *m*/*z* 253 and 255. In Fig. 2, the shifts with incident laser energy are more dramatic: at the lowest energy, spectrum (*a*), the major peak is $(M + 5H)^+$, changing to $(M + 2H)^+$ in spectrum (*b*), reducing in intensity in spectrum (*c*) and shifting to the $(M - H)^+$ ion at the highest energy, spectrum (*d*).

Figs. 3(*a*)–(*e*) show complete positive ion mass spectra of the polynuclear aromatic hydrocarbons pyrene, rubicene, pyranthrene, rubrene and fullerite respectively. Their molecular ion region relative intensities are listed in Table 1. The proportions of molecular ions, carbon cluster ions and aluminium ion (from the stub) vary from spectrum to spectrum. Figs. 3(*a*) and (*b*) show no significant Al peak; Figs. 3(*c*) and (*d*) show the Al ion as the most intense of the spectrum while Fig. 3(*e*), fullerite, shows only low intensity carbon cluster ions. The absence of a reduced molecular ion for fullerite indicates that the sample introduction method has removed solvent completely, since fullerenes are known to undergo protonation readily in chemical ionization studies.[14]

The positive ion pseudo molecular ions listed in Table 1 are not consistently M^+, $(M + H)^+$, $(M + 2H)^+$ or $(M + 3H)^+$; the most intense ion varies with laser power and with other factors, such as gas phase vapour pressure and depth of the ablation pit. The spectra from single laser pulses show the effect of laser energy, as has already been considered. Some of the observed ions can be attributed to ^{13}C isotopomers, but in most cases, the ion at higher mass than the 100% intensity peak is at too high an intensity to be explained away as the isotope peak alone. The ^{13}C isotope peak can be estimated as (1.1 × carbon number)% of the major peak taken to be 100%. For benzo[*e*]pyrene, the isotope contribution at the mass higher than the 100% peak will be about 22%, that for dibenzopyrene will be 26% and that for rubicene will be 28%; the peak intensities listed for these compounds in Table 1 are generally greater than the isotope contribution alone. The use of deuteriated solvents indicates quite clearly that the protonation in the ablation step comes from the aromatic structure itself

---

* The series of mass spectra were all done on the same target, on the same day, with the same mass calibration of the instrument. The instrument operator noted the effect of topography on spot size by viewing the sample through a microscope using a visible light beam, and having selected appropriate topographies, fired the Nd:YAG laser at each site. The fragment peaks (carbon clusters and the Al ion were detected) were all at the expected masses, confirming that the instrument calibration was unchanged.

† 5,6,11,12-Tetraphenylnaphthacene.

Table 1 Laser desorption mass spectra—positive ions; relative intensities of peaks in the molecular ion (M) region

Compound name (molec. mass)	−1	M	+1	+2	+3	+4	+5	+6	+7
Phenanthrene (178)	6	14	100	73	14	3	—	—	—
Pyrene (202)	—	4	17	100	45	17	—	—	—
Chrysene (228)	5	34	5	100	39	—	—	—	—
Benzo[*e*]pyrene (252)	[a] 7	32	27	100	66	20	4	—	—
	[b] —	15	11	100	79	18	5	—	—
	[b] —	22	10	100	51	15	—	—	—
	[b] —	—	50	—	100	—	—	—	—
	[c] 10	41	25	100	29	9	—	—	—
	[d] 10	55	24	100	67	14	—	—	—
	[e] 6	29	29	100	63	24	—	—	—
	[f] —	23	7	100	28	16	5	—	—
	[g] 5	36	19	100	51	15	—	—	—
Dibenzopyrene (302)	[a] 9	22	15	100	69	13	32	14	—
	[b] —	4	3	2	21	7	100	43	7
	[b] —	18	15	100	68	13	—	6	—
	[b] —	27	6	100	64	18	—	—	—
	[b] 100	—	—	—	—	—	—	—	—
	[c] —	11	6	100	43	—	—	—	—
	[d] —	33	10	100	43	10	—	—	—
	[e] —	34	12	100	83	12	—	—	—
	[f] —	22	16	100	66	25	—	—	—
	[g] —	30	21	100	71	10	—	—	—
Rubicene (326)	[a] 5	19	11	100	40	7	1	—	—
	[c] 21	100	14	93	57	21	—	—	—
	[d] 21	29	21	100	50	14	—	—	—
	[e] —	39	22	100	48	13	—	—	—
	[e] —	20	7	100	43	10	—	—	—
	[f] 10	36	12	100	23	11	2	—	—
	[g] —	23	8	100	41	8	3	—	—
	[h] 13	15	100	46	13	—	—	—	—
	[h] 7	21	4	100	54	14	—	—	—
	[h] 5	22	20	100	40	12	2	—	—
	[i] 8	23	8	100	67	23	8	—	—
Pyranthrene (376)	17	100	82	11	—	2	—	—	—
	50	100	59	44	—	—	—	—	—
Rubrene (532)	—	7	75	100	33	7	7	13	—
	7	—	7	100	83	41	17	3	
Fullerite									
Fullerene C_{60} (720)	100	19[j]	7[k]						
Fullerene C_{70} (840)	100	53[j]	21[k]						

---

[a] Manually summed spectra (10 for benzo[*e*]pyrene and dibenzopyrene, 13 for rubicene). [b] Laser power levels increase down the Table. [c] Solvent was sinapinic acid and toluene. [d] Solvent was toluene. [e] Solvent was $[^2H_8]$toluene. [f] Solvent was benzene. [g] Solvent was $[^2H_6]$benzene. [h] Glycerol used as liquid matrix. [i] Aluminium stub. [j] M − 24 ion. [k] M − 48 ion.

Table 2 Electron impact mass spectra; relative intensities of the molecular ion region

Compound	*m*/*z*	At. Comp.	−2	−1	M	+1	+2	+3	+4	+5
Phenanthrene	178	$C_{14}H_{10}$	16	9	100	15	1	—	—	—
			20[a]	12	100	15	—			
Pyrene	202	$C_{16}H_{10}$	18	20	100	20	2	—	—	—
			15[a]	10	100	20	—			
Chrysene	228	$C_{18}H_{12}$	21	10	100	20	2	—	—	—
			20[a]	8	100	20	—			
Perylene	252	$C_{20}H_{12}$	16	8	100	22	2	—	—	—
			22[a]	7	100	22	—			
Dibenzopyrene	302	$C_{24}H_{14}$	44	20	100	26	3	—	—	—
Rubicene	326	$C_{26}H_{14}$	24	9	100	29	4	—	—	—
Pyranthrene	376	$C_{30}H_{16}$	16	10	100	38	44	17	15	5

[a] These values from *The Eight Peak Index of Mass Spectra*, ref. 25.

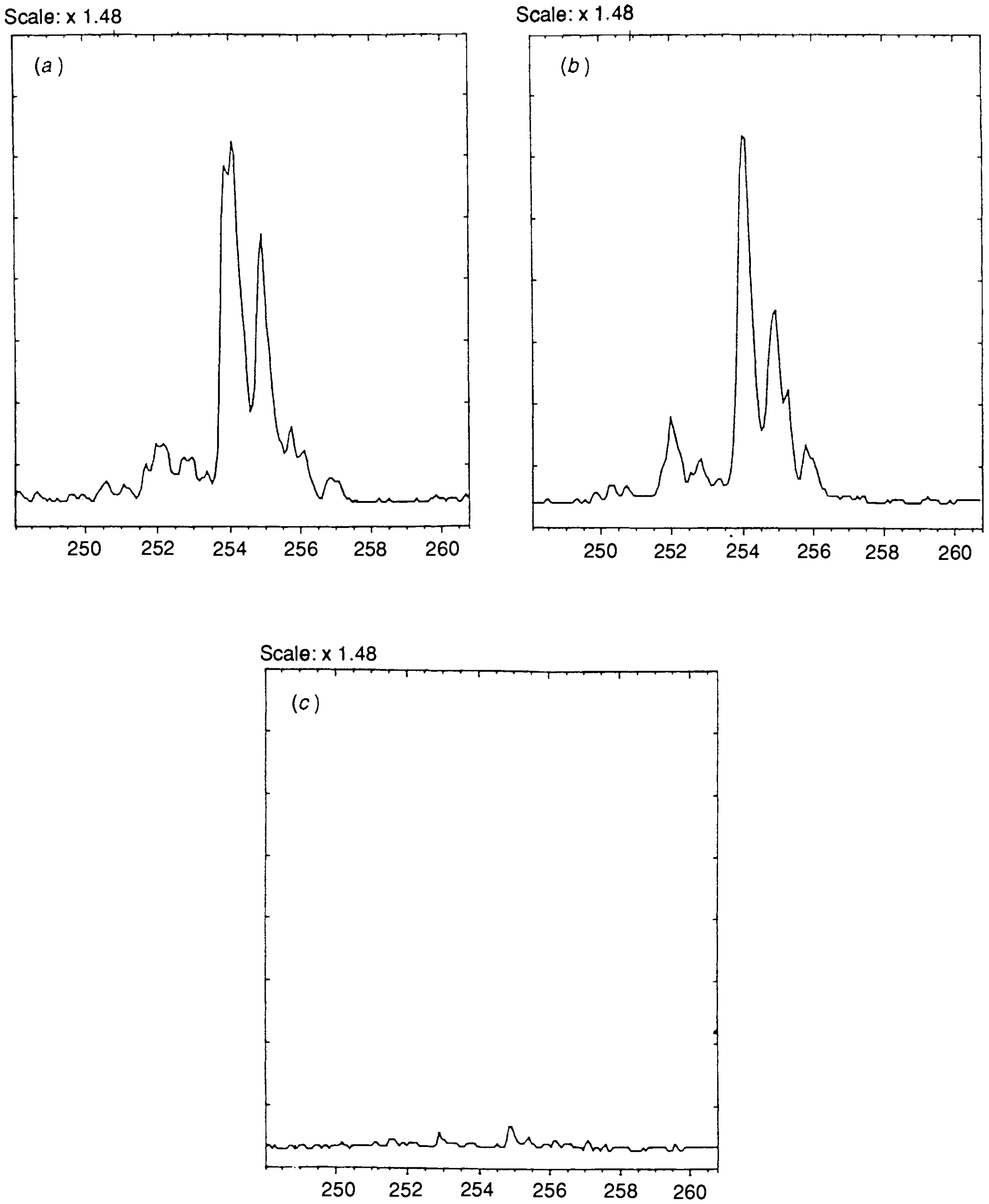

Fig. 1 Changes in the molecular ion region, positive ion laser desorption spectra, with laser energy for benzo[*e*]pyrene. Laser power increases from (*a*) to (*c*); for each spectrum, the most intense peak has been shown in Table 1 as 100% with the other peak intensities relative to it. Plots are of ion intensity *vs.* ionic mass (m/z)/u.

rather than from residual solvent. If this were not so, we would expect to see deuteriated molecular ions when using perdeuteriobenzene and perdeuterio-toluene, and to observe a change in the different rates of reaction with benzene and the methyl group of toluene. Shifts of relative intensities of pseudo-molecular ions are observed in Table 1, but the values using deuteriated solvents lie close to the values for protonated solvents. Similarly, the use of glycerol and sinapinic acid as matrices, has no clear influence on the pseudo-molecular ion intensities. One of the three rubicene spectra (Table 1) using glycerol as matrix shows the most intense ion as $(M + H)^+$ rather than as $(M + 2H)^+$, but this appears to be an effect of the low intensity of the molecular ion region (relatively high laser energy) in this case. Further work is required to allow us to establish the effects of isomeric shapes of these planar molecules on the relative intensities of pseudo molecular ions.

The fullerite spectra were generated from a solution initially in toluene and protonation would only be possible from retained solvent in the target crystals. The chemical ionization mass spectra of fullerene have been shown[14] to consist of series of highly protonated peaks, depending on the reagent molecule, indicating that the fullerene structures are extremely reactive under ion–molecule reaction conditions. In this work, only the fragment peaks from the loss of 24 or 48 mass units were detected in addition to the molecular ions and carbon clusters at low mass; this was demonstrated by the careful checking of the mass scale and expansion of the molecular ion region of the spectrum. The resolving power of the instrument is not sufficient to completely separate M^+ from $(M + 1)^+$, but a partial separation can be observed. Whilst the chemistry of C_{60} and C_{70} are distinct from the chemistry of compounds likely to be present in coals, fullerenes can be formed by the laser ablation of coal[10] and coals extracts[22] at high laser fluences and can coalesce[23] to form larger structures under mass spectrometric conditions; fullerenes have been found in nature only in a Russian Precambrian rock.[24] The complete absence in this

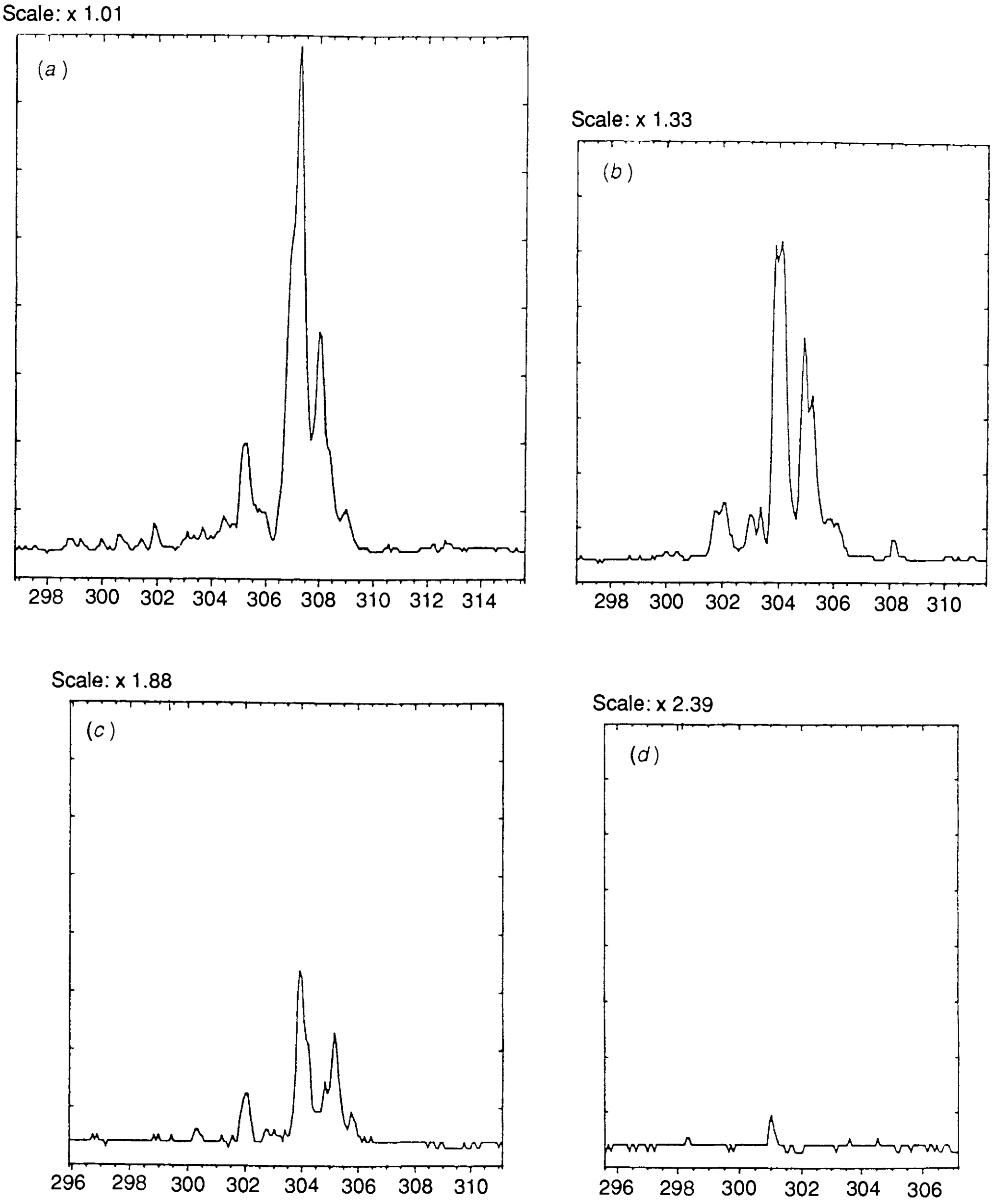

Fig. 2 Changes in the molecular ion region, positive ion laser desorption spectra, with laser energy for dibenzopyrene. Laser power increases from (*a*) to (*d*); for each spectrum, the most intense peak has been shown in Table 1 as 100% with the other peak intensities relative to it. Scale factors refer to an increased magnification compared with the overall spectrum. Plots are of ion intensity *vs.* ionic mass (*m*/*z*)/u.

work of any ions of mass greater than the molecular ions of the fullerenes is of particular importance to our work using coal and materials derived from coal where we have interpreted the high mass molecular ions detected to represent molecules which existed in the sample before ablation. No cluster ions of the type M_nH^+ have been detected in this work for any of the standard compounds.

Negative ion mass spectra of aromatics were characterized by a virtually complete absence of molecular ions; the summed relative intensities of molecular ions were less than 1% of the total ionization. A range of carbon cluster fragments was evident in the negative ion spectra. The energetics of electron capture during the ion molecular reactions taking place in the ablation mechanism are clearly not favourable. Fig. 4(*a*)–(*e*) show negative ion mass spectra of the polynuclear aromatic hydrocarbons benzo[*e*]pyrene, dibenzopyrene, pyranthrene, rubrene and fullerite respectively. The fullerite mixture gave some low intensity molecular ions, but the major feature of the spectrum was the series of carbon cluster ions below 200 u.

The positive ion electron impact spectra summarized in Table 2 show the molecular ion as the most intense ion for all the polyaromatics studied. Sample purity can be considered in relation to electron impact ionization, where molecular ion formation is related to purity. Pyranthrene shows evidence for components at masses 378 and 380 as impurities; the laser desorption spectra in Table 1 are anomalous in giving M^+ as the most intense ion. Rubrene did not give an adequate spectrum by electron impact, presumably because the maximum probe temperature was not high enough; the laser desorption spectral data in Table 1 suggest that its purity was high because it gave $(M + 2H)^+$ ions as the most abundant, in common with other pure aromatics. The rubrene crystals certainly looked regular and clear red in colour. Table 2 contains ion intensities taken from the Eight Peak Index,[25] where they are available; in general the measured spectra match those of the Index.

The discussion has concentrated on the formation of molecular ions because the thrust of our on-going work aims to identify the large molecular mass ions found in laser desorption spectra of material derived from coal. However, the carbon

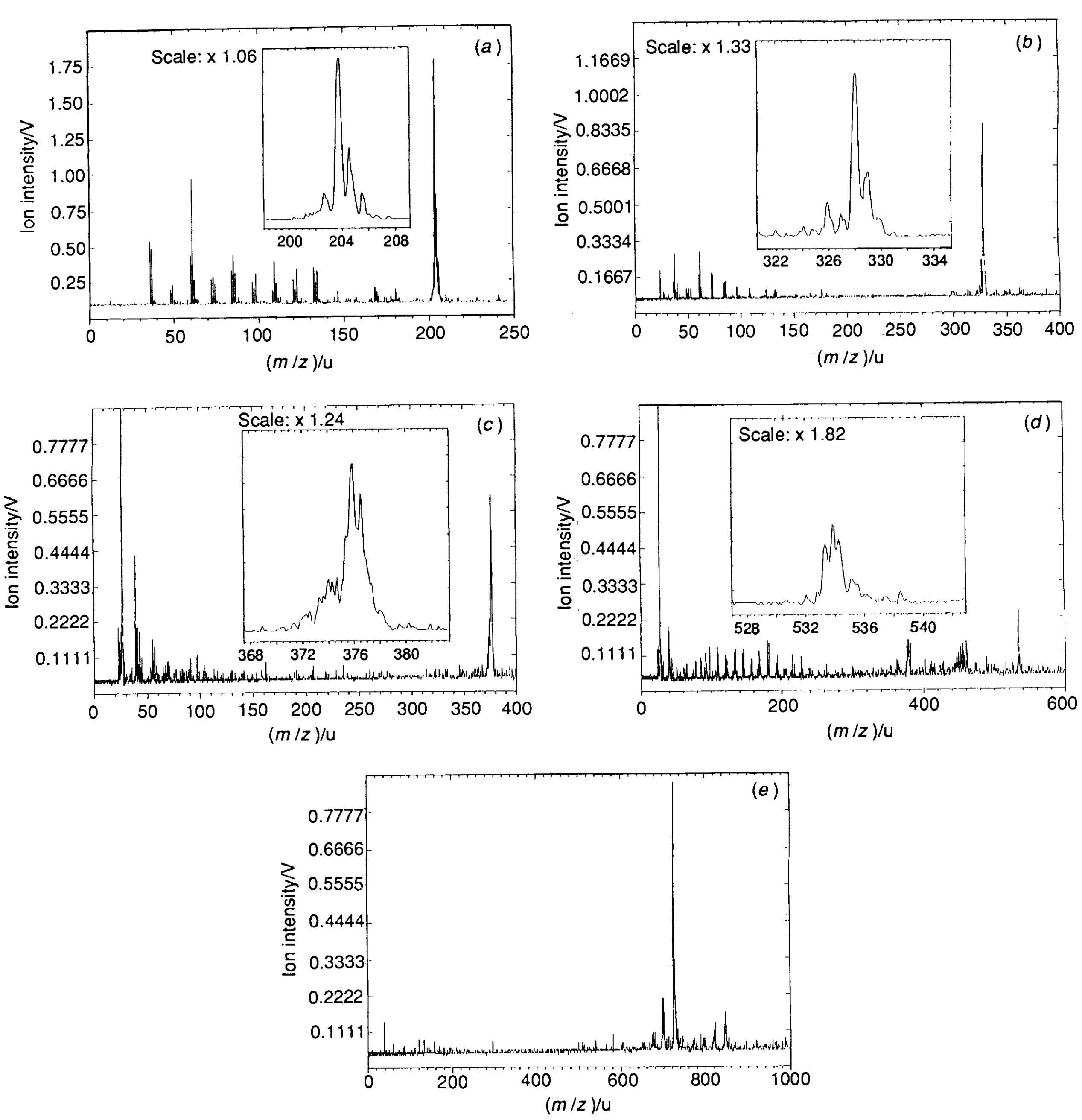

Fig. 3 (*a*)–(*e*) Complete positive ion laser desorption mass spectra of the polynuclear aromatic hydrocarbons pyrene, rubicene, pyranthrene, rubrene and fullerite respectively. Insert boxes show the molecular ion region expanded and magnified slightly. Plots are of ion intensity *vs.* ionic mass (*m*/*z*)/u.

clusters formed in every laser desorption spectrum deserve some mention. We have considered elsewhere their relation to the generation of fullerenes from carbon sources.[26] In this work, the intensities of the carbon cluster ions show an inverse relationship to molecular ion intensity as the laser power varies. Table 1 shows the variation of molecular ion ratio with laser power for benzo[*e*]pyrene and dibenzopyrene, with power increasing down the Table. The relative intensity changes as laser power increases, reflect the decreasing ion intensity of the molecular ion region and the increasing ion intensity of the carbon cluster region. Where the ablation pit reaches the metal target through the sample, the carbon clusters are less prominent and a large Al peak is evident (Al^+ and Al_2^+). For the four spectra from dibenzopyrene at increasing effective laser energy in Table 1 and Fig. 2, the sum of carbon cluster ions and aluminium ions increases from 71% of total ionization at the lowest energy to 99.8% at the highest energy.

A feature of the negative ion clusters is that the even carbon number clusters are more intense than the odd carbon number clusters and they form intense hydrogenated derivatives as $(C_nH_{1-3})^-$ whereas the odd carbon number clusters do not; this behaviour has been noted elsewhere[27] in the formation of carbon anion clusters from graphite in reaction with water vapour.

Conclusions

This work using a single laser for desorption and ionization has shown that positive ion–molecule reactions in the desorbing plume of material lead to successive hydrogenations of the molecular ions, with addition of up to seven hydrogen atoms, even though low laser power was used.

Negative molecular ions are not prominent for any of the aromatics studied and give only minor peaks in the fullerene spectra.

Apart from the hydrogenated positive ions, no adduct ions

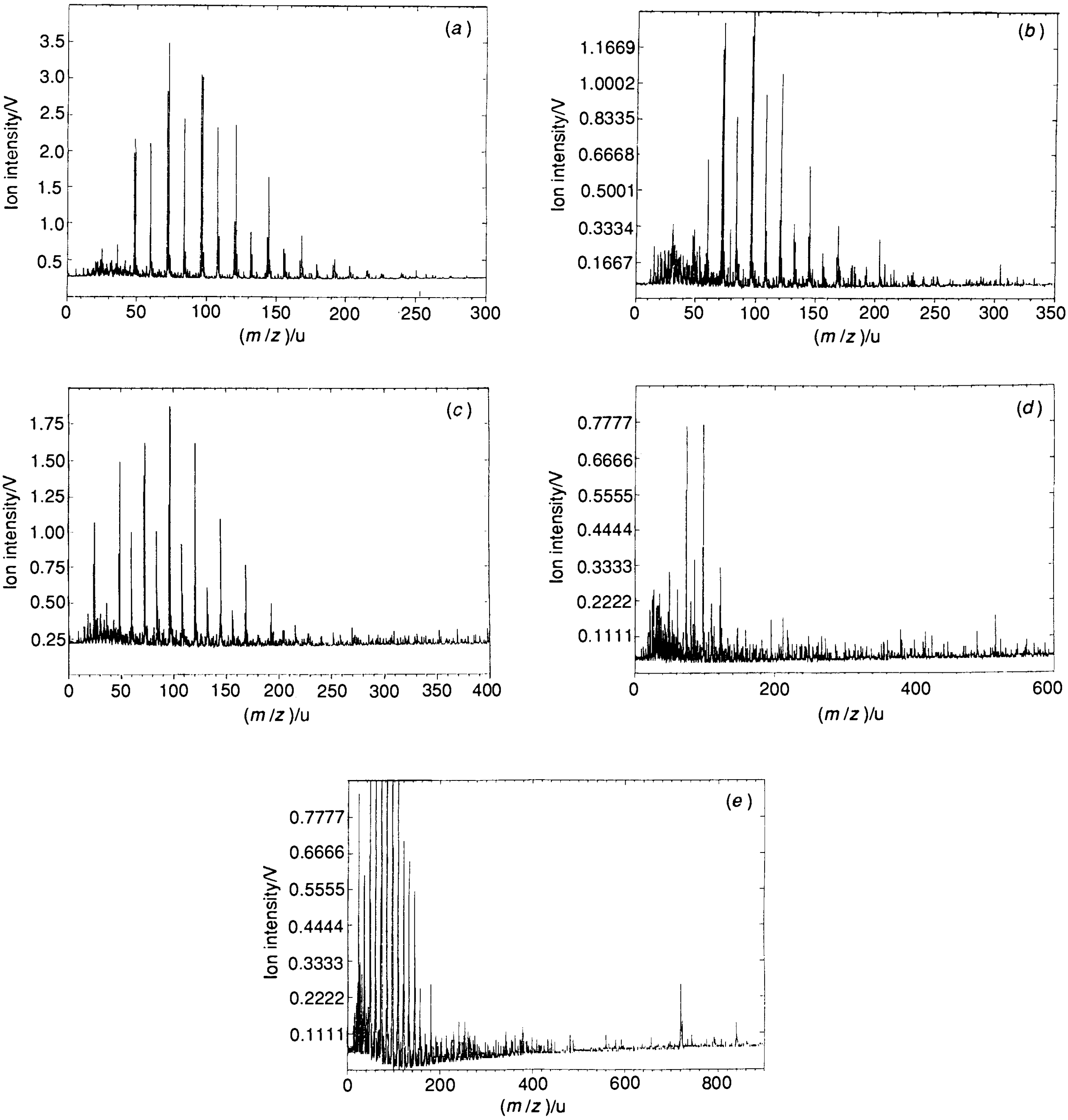

Fig. 4 (*a*)–(*e*) Negative ion laser desorption mass spectra of the polynuclear aromatic hydrocarbons benzo[*e*]pyrene, dibenzopyrene, pyranthrene, rubrene and fullerite respectively; plots are of ion intensity *vs.* ionic mass $(m/z)/\mathrm{u}$.

or ions of mass significantly greater than the molecular masses of the original aromatic compounds studied, have been detected.

The relative intensities of peaks in the laser generated mass spectra depend on the local laser energy absorbed per unit area and this changes with the topography of the crystalline sample surface for typical laser spot diameters of 2–5 um.

Carbon cluster ions, positive and negative, have been detected for all the compounds studied; these are thought to correspond to pyrolytic fragments generated during the desorption step.

Acknowledgements

We thank the British Coal Utilization Research Association Ltd. and the UK Department of Trade and Industry for a grant in aid of this research. The views expressed are those of the authors and not necessarily those of BCURA or the DTI. We also thank the British Coal Corporation for permission to publish and thank Dr. P. Burchill of British Coal for helpful comments.

References

1 F. Hillenkamp, M. Karas, R. C. Beavis and B. T. Chait, *Anal. Chem.*, 1991, **63**, 1193A.
2 S. Zhao, K. V. Somayajula, A. G. Sharkey, D. M. Hercules, F. Hillenkamp, M. Karas and A. Ingendoh, *Anal. Chem.*, 1991, **63**, 450.
3 U. Bahr, A. Deppe, M. Karas and F. Hillenkamp, *Anal. Chem.*, 1992, **64**, 2866.
4 J. P. Speir and I. J. Amster, *Anal. Chem.*, 1992, **64**, 1041.
5 I. Lee, T. A. Callcott and E. T. Arakawa, *Anal. Chem.*, 1992, **64**, 476.
6 A. J. Kubis, S. K. Viswanadham, A. G. Sharkey and D. M. Hercules, *Microbeam Anal.*, 1989, 364.
7 A. J. Kubis, K. V. Somayajula, A. G. Sharkey and D. M. Hercules, *Anal. Chem.*, 1989, **61**, 2516.

8 C. R. Dewey and R. W. Finney, *Anal. Proc.*, 1990, **27**, 125.

9 K. L. Busch, *J. Planar Chromatogr.*, 1992, **5**, 72.

10 P. F. Greenwood, M. G. Strachan, G. D. Willett and M. A. Wilson, *Org. Mass Spectrom.*, 1990, **25**, 353.

11 K. Balasanmugam, S. K. Viswanadhan and D. M. Hercules, *Anal. Chem.*, 1986, **58**, 1102.

12 M. L. Alexander, P. H. Hemberger, M. E. Cisper and N. S. Nogar, *Anal. Chem.*, 1993, **65**, 1609.

13 P. F. Greenwood, I. G. Dance, K. J. Fisher, G. D. Willett, L. S. K. Pang and M. A. Wilson, *Org. Mass Spectrom.*, 1991, **26**, 920.

14 D. Schroder, D. K. Bohme, T. Weiske and H. Schwarz, *Int. J. Mass Spectrom. Ion Processes*, 1992, **116**, R13.

15 C. Koster, M. Dey, J. Linder and J. Grotemeyer, in *Analytical Applications of Spectroscopy*, *Vol. II*, eds. A. M. C. Davies and C. S. Creaser, Royal Society of Chemistry, London, Cambridge, 1991, p. 113.

16 L. J. Kovalenko, C. R. Maechling, S. J. Clemett, J.-M. Philippoz and R. N. Zare, *Anal. Chem.*, 1992, **64**, 682.

17 R. Zenobi, J.-M. Philippoz, R. N. Zare, M. R. Wing, J. L. Bada and K. Marti, *Geochim. Cosmochim. Acta*, 1992, **56**, 2899.

18 P. John, C. A. F. Johnson, J. E. Parker, G. P. Smith, A. A. Herod, A. F. Gaines, C.-Z. Li and R. Kandiyoti, *Rapid Commun. Mass Spectrom.*, 1991, **5**, 364.

19 J. E. Parker, C. A. F. Johnson, P. John, G. P. Smith, A. A. Herod, B. J. Stokes and R. Kandiyoti, *Fuel*, 1993, **72**, 1381.

20 A. A. Herod, R. Kandiyoti, J. E. Parker, C. A. F. Johnson, P. John, G. P. Smith and C.-Z. Li, *J. Chem. Soc., Chem. Commun.*, 1993, 767.

21 L. D. Detter, O. W. Hand, R. G. Cooks and R. A. Walton, *Mass Spectrom. Rev.*, 1988, **7**, 465.

22 J. A. Burroughs, B. M. Cadre and L. Hanley, *Proc. Conf. ASMS, 41st*, San Francisco, 28th May–3rd June 1993.

23 C. Yeretzian, K. Hansen, F. Diederich and R. L. Whetten, *Nature*, 1992, **359**, 44.

24 P. R. Buseck, S. J. Tsipursky and R. Hettich, *Science*, **257**, 215, 1992.

25 *The Eight Peak Index of Mass Spectra*, 3rd edn., Royal Society of Chemistry, London.

26 A. A. Herod, R. Kandiyoti, J. E. Parker, C. A. F. Johnson, P. John, G. P. Smith and C.-Z. Li, *Rapid Commun. Mass Spectrom.*, 1993, **7**, 360.

27 C. Q. Jiao, D. K. Phelps, S. Lee, Y. Huang and B. S. Freiser, *Rapid Commun. Mass Spectrom.*, 1993, **7**, 404.

Paper 3/06090J
Received 12*th October* 1993
Accepted 1*st November* 1993